Temporal photonic crystals with modulations of both permittivity and permeability

Juan Sabino Martínez-Romero,* O. M. Becerra-Fuentes,† and P. Halevi‡
Instituto Nacional de Astrofísica, Óptica y Electrónica Tonantzintla, 72840 Puebla, Mexico
(Received 20 January 2016; published 9 June 2016)

We present an in-depth study of electromagnetic wave propagation in a *temporal* photonic crystal, namely, a nonconducting medium whose permittivity $\varepsilon(t)$ and/or permeability $\mu(t)$ are modulated periodically by unspecified agents (these modulations not necessarily being in phase). Maxwell's equations lead to an eigenvalue problem whose solution provides the dispersion relation $\omega(k)$ for the waves that can propagate in such a dynamic medium. This is a generalization of previous work [J. R. Zurita-Sánchez and P. Halevi, Phys. Rev. A **81**, 053834 (2010)] that was restricted to the electric modulation $\varepsilon(t)$. For our numerical work (only) we assumed the harmonic modulations $\varepsilon(t) = \bar{\varepsilon}[1 + m_\varepsilon \sin(\Omega t)]$ and $\mu(t) = \bar{\mu}[1 + m_\mu \sin(\Omega t + \theta)]$, where Ω is the circular modulation frequency; m_ε and m_μ are, respectively, the strengths of the electric and magnetic modulations; and θ is the phase difference between these modulations. An analytic calculation for weak modulations ($m_\varepsilon \ll 1, m_\mu \ll 1$) leads to two k bands, $k_1(\omega)$ and $k_2(\omega)$, that are separated by a k gap. If the modulations are in phase ($\theta = 0$), this gap is proportional to $|m_\varepsilon - m_\mu|$, while the gap is proportional to $(m_\varepsilon + m_\mu)$ if the modulations are out of phase ($\theta = \pi$). The gap thus disappears for equal, in-phase, modulations ($m_\varepsilon = m_\mu$). An exact solution of the eigenvalue equation confirms that these approximations hold reasonably well even for moderate modulations. In fact, there are no k gaps for equal modulations even if these are very strong ($m_{\varepsilon,\mu} \lesssim 1$). The photonic band structure $k(\omega)$ is periodic in ω, with period Ω, and there is an infinite number of bands $k_1(\omega)$, $k_2(\omega)$, ... Further, by allowing $\varepsilon(t)$ and $\mu(t)$ to have imaginary parts, we examined the effects of damping [Im $k(\omega)$] on the k bands. We also determined the optical response of a temporal photonic crystal slab, applying the above harmonic model for $\varepsilon(t)$ and $\mu(t)$. The reflected and transmitted light represent a frequency comb of frequencies ω, $|\omega \pm \Omega|$, $|\omega \pm 2\Omega|$, ... The transmission coefficients $\mathcal{T}_n(\omega)$ for these harmonics $n\Omega$ of the modulation frequency strongly depend on the parameters m_ε, m_μ, and θ, as well as on the thickness of the slab. Moreover, they can much exceed unity, as a result of energy transfer from the source of modulation. In a particularly interesting case, $\mathcal{T}_n(\omega)$ exhibits oscillations with peaks that resemble parametric resonances, rather than the usual Fabry-Perot resonances.

DOI: 10.1103/PhysRevA.93.063813

I. INTRODUCTION

Tuning and modulation of material media and metamaterials are topics of intensive interest, with the expectation of varied applications. It has been posited that modulation of the permittivity could lead to many exotic effects: resonant cavity photon creation via the dynamic Casimir effect [1]; the stopping and time-reversal of light [2]; complete optical isolation [3] and other topological effects [4]; transitions between discrete modes of a silicon optical microcavity, achieved by ultrafast tuning of the refractive index of the cavity [5]; and the photonic Aharonov-Bohm effect [6]. Moreover, a split-ring resonator can be converted into a dynamic element by placing in its capacitive gap a varactor or a nonlinear material. Such a metamaterial can be then externally modulated by means of an ac voltage or intense pulses. This can be exploited to achieve several important effects: switching the properties of the substrate material by THz or GHz pulses [7], phase conjugation and negative refraction [8], and parametric oscillations [9]. Very recently, it was demonstrated that a moderately intense laser pulse can modulate the dielectric constant of a molecular monolayer, adsorbed on a metallic substrate, by as much as 10%, returning the monolayer to its initial state after the pulse [10].

The importance of tuning metamaterials is evidenced by the numerous reviews on this subject [11]. In particular, Kozyrev *et al.* [12] achieved parametric amplification in distributed high-pass transmission lines that exhibited metamaterial behavior. Employing (nonlinear) varactors, the same group [13] also reported other interesting features: harmonic and subharmonic generation, modulational instabilities, and envelope solitons. Further, English *et al.* [14] showed experimentally and numerically that stable localized modes can be produced in a nonlinear bandpass transmission line. Gorkunov and Lapine [15] studied a metamaterial slab composed of an array of split-ring resonators tuned by an external microwave magnetic field.

In the past few years, one of the authors (P.H.) and collaborators have studied theoretically the behavior of a medium whose permittivity $\varepsilon(t)$ is a periodic function of time, terming such a dynamic medium a "*temporal* photonic crystal" (TPC). A TPC exhibits wave vector k (or propagation constant β) gaps, and, upon excitation with monochromatic light, the reflected light and the transmitted light take the form of a frequency comb with the spacing equal to the modulation frequency [16]. The latter behavior has also been reported for surface plasmons in a thin oscillating piezoelectric film inside a metallic waveguide [17]. Further, we have shown that a TPC displays parametric resonances that are subject to a special geometric condition [18]. Also, a pulse transmitted through a TPC slab separates into harmonics of the modulation

*jsmr@inaoep.mx
†olga.m.becerra.fuentes@intel.com
‡halevi@inaoep.mx

frequency, and it turns out that the peaks of these harmonics can emerge on the other side faster than light in vacuum [19].

The study of TPCs is challenging and results in interesting new physics. However, it is difficult to achieve appreciable modulations with dielectric materials in the optical regime. An attractive alternative, though, is provided by a dynamic transmission line (DTL) where it is easy to obtain high modulations of the parameters in the microwave region at modulation frequencies $\Omega/2\pi$ on the order of the signal frequency $\omega/2\pi$. With the proper choice of parameters, a DTL can mimic a TPC in the long wavelength limit and hence can reproduce all the interesting effects predicted for the TPC. Indeed, very recently we fabricated such a DTL and demonstrated experimentally the existence of a $k(\beta)$ gap [20]. In our experiment, the dependence on time of the capacitance $C(t)$ was realized by varactors that are all fed *in tandem* by identical modulation voltages. By choosing $C(t)/a = \varepsilon(t)$, where a is the length of the unit cell of the DTL, and $L/a = \mu$ (relating the inductance L and the permeability μ), the DTL mimics the TPC very well for $ka \ll 1$. This correspondence is, however, imperfect because the imaginary parts attributed to ε and μ (see Sec. IV B) cannot mimic perfectly the complex resistive effects in a transmission line [21]. We also measured the harmonics $\Omega - \omega$ of the excitation frequency ω and beats for $\omega \simeq \Omega/2$ [21].

In the present paper, we generalize the concept of the TPC to periodic modulation of the permeability $\mu(t)$, in addition to modulation of the permittivity $\varepsilon(t)$. As will be shown, the dispersion relation or photonic band structure $k(\omega)$ depends qualitatively on the modulation strengths m_ε and m_μ of $\varepsilon(t)$ and $\mu(t)$, the widths of the k gaps being roughly proportional to $|m_\varepsilon - m_\mu|$. We note that these effects should be observable in a DTL with a modulated inductance $L(t)$, as well as a modulated capacitance $C(t)$, in every unit cell.

In the next section we derive the eigenvalue equation for the Fourier coefficients of the electric field in the bulk TPC. It is solved analytically, assuming weak modulations $m_\varepsilon \ll 1$ and $m_\mu \ll 1$, in Sec. III. An exact numerical calculation provides the photonic band structures for both the lossless and the lossy media (see Sec. IV). Then, in Sec. V, we investigate the transmission of light through a TPC slab, and we conclude the paper in Sec. VI.

II. FROM MAXWELL'S EQUATIONS TO THE EIGENVALUE EQUATION

This paper concerns a boundless, uniform, isotropic, and dispersionless medium. It is distinguished by its electric and magnetic properties both being dynamic; specifically, we assume that the permittivity $\varepsilon(t)$ and the permeability $\mu(t)$ are periodic functions of time. Hence, the constitutive relations for the fields are $\mathbf{D}(\mathbf{r},t) = \varepsilon(t)\mathbf{E}(\mathbf{r},t)$ and $\mathbf{B}(\mathbf{r},t) = \mu(t)\mathbf{H}(\mathbf{r},t)$. The relevant Maxwell's equations are then

$$\nabla \times \mathbf{E}(\mathbf{r},t) = -\frac{\partial}{\partial t}[\mu(t)\mathbf{H}(\mathbf{r},t)], \tag{1a}$$

$$\nabla \times \mathbf{H}(\mathbf{r},t) = \frac{\partial}{\partial t}[\varepsilon(t)\mathbf{E}(\mathbf{r},t)]. \tag{1b}$$

Eliminating the magnetic field $\mathbf{H}$ we get the wave equation for the electric field $\mathbf{E}$:

$$\nabla^2 E - \frac{1}{c^2}\frac{\partial}{\partial t}\left\{\mu_r(t)\frac{\partial}{\partial t}[\varepsilon_r(t)E]\right\} = 0, \tag{2}$$

where $\varepsilon(t) = \varepsilon_0\varepsilon_r(t)$, $\mu(t) = \mu_0\mu_r(t)$, and $c = (\varepsilon_0\mu_0)^{-1/2}$ is the speed of light in vacuum. The medium being uniform, it must have plane wave solutions, namely $\mathbf{E}(\mathbf{r},t) = \mathbf{E}(t)\exp(i\mathbf{k}\cdot\mathbf{r})$, where $\mathbf{k}$ is the wave vector. Then Eq. (2) reduces to

$$k^2c^2E(t) + \frac{d}{dt}\left\{\mu_r(t)\frac{d}{dt}[\varepsilon_r(t)E(t)]\right\} = 0. \tag{3}$$

Now assuming that the relative permittivity $\varepsilon_r(t)$ and the relative permeability $\mu_r(t)$ are periodic functions, these can be expanded in complex Fourier series:

$$\varepsilon_r(t) = \sum_m \varepsilon_m e^{im\Omega t}, \tag{4}$$

$$\mu_r(t) = \sum_l \mu_l e^{il\Omega t}. \tag{5}$$

Here, Ω is the circular modulation frequency, namely, $\Omega = 2\pi/T$, where T is the period of both $\varepsilon_r(t)$ and $\mu_r(t)$. Equatio (3) is solved by the Bloch-Floquet theorem, which implies that $E(t)$ is a superposition of harmonic oscillations of frequencies $\omega - n\Omega$, n running over all integers:

$$E(t) = \sum_n e_n(\omega)e^{-i(\omega-n\Omega)t}. \tag{6}$$

Here, ω can be defined as the "Bloch frequency," akin to the "Bloch wave vector" in the case of spatial periodicity. It plays the role of an arbitrary excitation frequency.

Substituting Eqs. (4)–(6) in Eq. (3) we get that

$$k^2c^2\sum_n e_n e^{in\Omega t} - \sum_{l,m,n}\mu_l\varepsilon_m e_n[\omega - (l+m+n)\Omega] \times [\omega - (m+n)\Omega]e^{i(l+m+n)\Omega t} = 0.$$

This equation is satisfied at any instant of time t provided that

$$k^2c^2e_n - \sum_{l,m}\mu_l\varepsilon_m e_{n-l-m}(\omega - n\Omega)[\omega - (n-l)\Omega] = 0 \tag{7}$$

for all n. Manipulating the indices l, m, and n one can find that

$$\sum_{m,n}[\mu_{l-m}\varepsilon_{m-n}(\omega - l\Omega)(\omega - m\Omega) - k^2c^2\delta_{ln}\delta_{m0}]e_n(\omega) = 0, \quad l = 0, \pm 1, \pm 2, \ldots, \tag{8}$$

where δ_{ln} is the Kronecker delta function. Equation (8) is our eigenvalue equation. It is a set of an infinite number of linear equations for an infinite number of eigenfunctions $e_n(\omega)$; these are the field amplitudes in Eq. (6). The eigenvalues $k(\omega)$ or $\omega(k)$ are gotten by requiring that the determinant of the coefficients of the $e_n(\omega)$ vanishes. These eigenvalues constitute the photonic band structure that is characteristic of the plane waves that can propagate in a medium with periodically modulated permittivity and permeability. It is instructive first to study the analytic solutions of Eq. (8) that can be derived for weak modulation.

III. WEAK MODULATION APPROXIMATION

If $\varepsilon(t)$ and $\mu(t)$ are weakly modulated then most harmonics $n\Omega$ of the modulation frequency in Eq. (8) contribute very little to the field $E(t)$. In order to judiciously select the important values of n, first we turn to the extreme assumption of vanishing modulation. In this limit $\varepsilon_r(t)$ and $\mu_r(t)$ reduce to their average values $\bar{\varepsilon}_r$ and $\bar{\mu}_r$, respectively, so that their Fourier coefficients in Eq. (8) are

$$\varepsilon_{m-n} = \bar{\varepsilon}_r \delta_{mn}, \tag{9}$$

$$\mu_{l-m} = \bar{\mu}_r \delta_{lm}. \tag{10}$$

Substitution in Eq. (8) gives

$$[\bar{\varepsilon}_r \bar{\mu}_r (\omega - l\Omega)^2 - k^2 c^2] e_l(\omega) = 0,$$

hence

$$\omega = l\Omega \pm kc/(\bar{\varepsilon}_r \bar{\mu}_r)^{1/2}, \quad l = 0, \pm 1, \pm 2, \ldots \tag{11}$$

For $l = 0$, the "+" and "−" solutions describe plain waves propagating to the "right" and to the "left" in a medium with the refractive index $(\bar{\varepsilon}_r \bar{\mu}_r)^{1/2}$. For $l \neq 0$, these straight dispersion lines of positive and negative slopes are displaced along the frequency axis by integer multiples of Ω. This is the result of the temporal periodicity and corresponds to the "empty *temporal* lattice" model, analogous to the "empty (spatial) lattice" model of Ref. [22].

Which are the most important partial modes that contribute? The answer depends on the ranges of interest of ω and k. Because small values of ω ($<\Omega$) and k [$<\Omega(\bar{\varepsilon}_r \bar{\mu}_r)^{1/2}/c$] are most easily accessed experimentally, our choices are

$$\omega = +kc/(\bar{\varepsilon}_r \bar{\mu}_r)^{1/2} \quad (\text{for} \quad l = 0) \tag{12}$$

and

$$\omega = \Omega - kc/(\bar{\varepsilon}_r \bar{\mu}_r)^{1/2} \quad (\text{for} \quad l = 1). \tag{13}$$

These modes intersect at $\omega = \frac{1}{2}\Omega$ and $k = \frac{1}{2}\Omega(\bar{\varepsilon}_r \bar{\mu}_r)^{1/2}/c$, suggesting strong interaction at the intersection point for finite modulations.

For weak modulation, the important harmonics are then $n\Omega = 0$ and $n\Omega = \Omega$ and hence we restrict all the integers (l,m,n) in Eq. (8) to the values 0 and 1. Now allowing for finite modulation, this equation reduces to the following set of two equations:

$$\begin{aligned}&[\bar{\varepsilon}_r \bar{\mu}_r \omega^2 - k^2 c^2 + \varepsilon_1 \mu_{-1} \omega(\omega - \Omega)] e_0(\omega) \\ &\quad + [\bar{\mu}_r \varepsilon_{-1} \omega^2 + \bar{\varepsilon}_r \mu_{-1} \omega(\omega - \Omega)] e_1(\omega) = 0,\end{aligned} \tag{14}$$

$$\begin{aligned}&[\bar{\varepsilon}_r \mu_1 \omega(\omega - \Omega) + \bar{\mu}_r \varepsilon_1 (\omega - \Omega)^2] e_0(\omega) + [\bar{\varepsilon}_r \bar{\mu}_r (\omega - \Omega)^2 \\ &\quad + \varepsilon_{-1} \mu_1 \omega(\omega - \Omega) - k^2 c^2] e_1(\omega) = 0.\end{aligned} \tag{15}$$

In the present approximation, the dispersion relation $\omega(k)$ is gotten from the requirement that the determinant of the coefficients of $e_0(\omega)$ and $e_1(\omega)$ vanishes. This gives rise to a quadratic equation for k^2, to which there correspond two solutions $k_\pm(\omega)$ for a given frequency and propagation direction.

Henceforth, we limit the generality to harmonic modulations:

$$\varepsilon_r(t) = \bar{\varepsilon}_r [1 + m_\varepsilon \sin(\Omega t)], \tag{16}$$

$$\mu_r(t) = \bar{\mu}_r [1 + m_\mu \sin(\Omega t + \theta)]. \tag{17}$$

Here, m_ε and m_μ are the strengths of the electric and magnetic modulations or, briefly, modulations. We also assume a phase difference θ between the magnetic and the electric modulations. Because of our assumption of weak modulation, we can expect the approximation to give reasonably accurate results for $0 \leqslant m_\varepsilon, m_\mu \ll 1$. It follows from Eqs. (16) and (17) that

$$\varepsilon_{\pm 1} = \pm m_\varepsilon \bar{\varepsilon}_r / 2i, \quad \mu_{\pm 1} = \pm m_\mu \bar{\mu}_r \exp(\pm i\theta)/2i. \tag{18}$$

The aforementioned quadratic equation then reduces to

$$\begin{aligned}&(k^2 c^2)^2 - \bar{\varepsilon}_r \bar{\mu}_r \left[\omega^2 + (\Omega - \omega)^2 - \tfrac{1}{2} m_\varepsilon m_\mu \cos\theta\, \omega(\Omega - \omega)\right] \\ &\quad \times (k^2 c^2) + \bar{\varepsilon}_r^2 \bar{\mu}_r^2 \left(1 - \tfrac{1}{4} m_\varepsilon^2 - \tfrac{1}{4} m_\mu^2 + \tfrac{1}{16} m_\varepsilon^2 m_\mu^2\right) \\ &\quad \times \omega^2 (\Omega - \omega)^2 = 0.\end{aligned} \tag{19}$$

The last equation shows that $\bar{\varepsilon}_r$ and $\bar{\mu}_r$ are interchangeable, and so are also m_ε and m_μ. Further, it is seen that $k(\omega) = k(\Omega - \omega)$, implying that the bands possess mirror symmetry about $\omega = \frac{1}{2}\Omega$. This suggests a gap between the k bands, $k_+(\frac{1}{2}\Omega) - k_-(\frac{1}{2}\Omega)$, at this frequency. In order to explore this possibility, now we restrict the calculation to $\omega = \frac{1}{2}\Omega$. Neglecting the extremely small term proportional to $m_\varepsilon^2 m_\mu^2$, the solution of Eq. (19) is

$$\begin{aligned}k^2 c^2 = \tfrac{1}{4} \bar{\varepsilon}_r \bar{\mu}_r \Omega^2 \big[1 - \tfrac{1}{4} m_\varepsilon m_\mu \cos\theta \\ \pm \tfrac{1}{2} \left(m_\varepsilon^2 - 2 m_\varepsilon m_\mu \cos\theta + m_\mu^2\right)^{1/2}\big].\end{aligned} \tag{20}$$

It follows that

$$k \simeq \frac{(\bar{\varepsilon}_r \bar{\mu}_r)^{1/2} \Omega}{2c} \left[1 \pm \frac{1}{4} \left(m_\varepsilon^2 - 2 m_\varepsilon m_\mu \cos\theta + m_\mu^2\right)^{1/2}\right]. \tag{21}$$

We conclude that there is a band gap:

$$\Delta k = k_+ - k_- \simeq \frac{(\bar{\varepsilon}_r \bar{\mu}_r)^{1/2} \Omega}{4c} \left(m_\varepsilon^2 - 2 m_\varepsilon m_\mu \cos\theta + m_\mu^2\right)^{1/2}. \tag{22}$$

The midpoint between $k_-(\frac{1}{2}\Omega)$ and $k_+(\frac{1}{2}\Omega)$ is

$$\bar{k} \simeq \frac{(\bar{\varepsilon}_r \bar{\mu}_r)^{1/2} \Omega}{2c}, \tag{23}$$

independent of the modulation in this approximation. Compactly, the relative gap is then

$$\frac{\Delta k}{\bar{k}} \simeq \frac{1}{2} \left(m_\varepsilon^2 - 2 m_\varepsilon m_\mu \cos\theta + m_\mu^2\right)^{1/2}. \tag{24}$$

The behavior strongly depends on the phase difference θ and on the modulations m_ε and m_μ. We consider three cases:

(a) $\theta = 0$,

$$\frac{\Delta k}{\bar{k}} \simeq \frac{1}{2} |m_\varepsilon - m_\mu|; \tag{25}$$

TABLE I. Comparison between accurate and approximate values of the normalized band gap $\Delta k/\bar{k}$ and the normalized midgap $\hat{\bar{k}} = \bar{k}c/\Omega(\bar{\varepsilon}_r\bar{\mu}_r)^{1/2}$ for the phase difference $\theta = 0$.

θ		Solutions of Eq. (28)		Eqs. (23)–(27)	
m_ε	m_μ	$\Delta k/\bar{k}$	$\hat{\bar{k}}$	$\Delta k/\bar{k}$	$\hat{\bar{k}}$
0.1	0.2	0.0512	0.4940	0.0500	0.5
0.1	0.3	0.1043	0.4888	0.1000	0.5
0.1	0.4	0.1611	0.4814	0.1500	0.5
0.2	0.3	0.0533	0.4838	0.0500	0.5
0.2	0.4	0.1103	0.4756	0.1000	0.5
0.3	0.4	0.0570	0.4679	0.0500	0.5
0.4	0.3	0.0570	0.4679	0.0500	0.5

(b) $\theta = \frac{\pi}{2}$ or $\frac{3\pi}{2}$,

$$\frac{\Delta k}{\bar{k}} \simeq \frac{1}{2}\left(m_\varepsilon^2 + m_\mu^2\right)^{1/2}; \tag{26}$$

(c) $\theta = \pi$,

$$\frac{\Delta k}{\bar{k}} \simeq \frac{1}{2}(m_\varepsilon + m_\mu). \tag{27}$$

We conclude that, if the electric and magnetic modulations are in phase ($\theta = 0$), then the k gap is proportional to the difference $|m_\varepsilon - m_\mu|$ of these modulations and thus disappears entirely ($\Delta k = 0$) for equal modulations ($m_\varepsilon = m_\mu$). On the other hand, if the modulations are out of phase, then the relative gap is equal to the arithmetic average of the two modulations.

In Sec. IV A we compare the predictions of the approximate Eqs. (23)–(27) with exact solutions of the eigenvalue problem; see Tables I–III. This confirms that these approximations are unexpectedly good.

IV. THE PHOTONIC BAND STRUCTURE

In this section we proceed to solve Eq. (8) numerically for the harmonic model of modulation introduced in Eqs. (16) and (17). Now, however, we do not restrict the modulations m_ε and/or m_μ to small values as we did in the previous section. The approximation assumed there led to two solutions, $k_-(\omega)$ and $k_+(\omega)$, for the wave vector k for every value of the frequency ω. Now we find that, actually, the number of solutions is infinite. Hence, it is convenient to label these solutions as $k_p(\omega)$, where $p = 1,2,3,\ldots$ in order of increasing value of k_p. Similary, the eigenfunctions are labeled as $e_{pn}(\omega)$. Then we rewrite Eq. (8) as

$$\sum_{m,n}\left[\hat{\mu}_{l-m}\hat{\varepsilon}_{m-n}(\hat{\omega}-l)(\hat{\omega}-m) - \hat{k}_p^2\delta_{ln}\delta_{m0}\right]e_{pn}(\hat{\omega}) = 0,$$
$$l = 0, \pm 1, \pm 2, \ldots, \tag{28}$$

where $\hat{\mu}_n = \mu_n/\bar{\mu}_r$ and $\hat{\varepsilon}_n = \varepsilon_n/\bar{\varepsilon}_r$, with $\bar{\mu}_r$ and $\bar{\varepsilon}_r$ being, respectively, the averages of $\mu_r(t)$ and $\varepsilon_r(t)$, and the normalized frequency $\hat{\omega}$ and the wave vector $\hat{k}_p$ are defined as

$$\hat{\omega} = \frac{\omega}{\Omega}, \tag{29}$$

$$\hat{k}_p = \frac{k_p c}{\Omega\sqrt{\bar{\varepsilon}_r\bar{\mu}_r}}. \tag{30}$$

It is readily seen (by shifting l, m, and n by 1) that $\hat{k}_p(\hat{\omega}+1) = \hat{k}_p(\hat{\omega})$ or

$$k(\omega + \Omega) = k(\omega). \tag{31}$$

This means that the entire band structure is periodic in the circular frequency, the period being the circular modulation frequency Ω. This periodicity mirrors, of course, the temporal periodicity of $\varepsilon(t)$ and $\mu(t)$, and, unlike the case of spatial periodicity, where the band structure is periodic in k (not, however, in ω), temporal modulation does not result in periodicity of the wave vector k.

TABLE II. Same as Table I but for the phase difference $\theta = \pi/2$.

θ		Solutions of Eq. (28)		Eqs. (23)–(27)	
m_ε	m_μ	$\Delta k/\bar{k}$	$\hat{\bar{k}}$	$\Delta k/\bar{k}$	$\hat{\bar{k}}$
0.1	0.1	0.0710	0.4983	0.0706	0.5
0.1	0.2	0.1131	0.4956	0.1118	0.5
0.1	0.3	0.1624	0.4912	0.1580	0.5
0.2	0.2	0.1435	0.4931	0.1414	0.5
0.2	0.3	0.1852	0.4886	0.1802	0.5
0.2	0.4	0.2348	0.4821	0.2236	0.5
0.4	0.2	0.2348	0.4821	0.2236	0.5

TABLE III. Same as Table I but for the phase difference $\theta = \pi$.

θ		Solutions of Eq. (28)		Eqs. (23)–(27)	
m_ε	m_μ	$\Delta k/\bar{k}$	$\hat{\bar{k}}$	$\Delta k/\bar{k}$	$\hat{\bar{k}}$
0.1	0.1	0.1003	0.4990	0.1000	0.5
0.1	0.2	0.1512	0.4972	0.1500	0.5
0.1	0.3	0.2040	0.4935	0.2000	0.5
0.1	0.4	0.2601	0.4877	0.2500	0.5
0.2	0.2	0.2019	0.4962	0.2000	0.5
0.2	0.3	0.2543	0.4933	0.2500	0.5
0.3	0.2	0.2543	0.4933	0.2500	0.5

A. Lossless medium

First we neglect losses, assuming that $\varepsilon_r(t)$ and $\mu_r(t)$ are real functions, in fact given by Eqs. (16) and (17). Due to the normalization procedure carried out in Eq. (28), the only parameters are the electric and magnetic modulations m_ε and m_μ and the phase difference θ between these modulations. In Figs. 1–5 we present the photonic band structures and band gaps for various values of these parameters. The periodicity with ω, according to Eq. (31), is explicit from the two periods shown in Figs. 1, 2, and 4. In the case of Fig. 1, the modulations are in phase ($\theta = 0$) and m_ε is larger than m_μ. For every value of $\hat{\omega}$ there is an infinite number of solutions $\hat{k}(\omega)$, namely, $\hat{k}_1(\hat{\omega})$, $\hat{k}_2(\hat{\omega})$, etc. The salient feature is a wide gap $\Delta\hat{k}_{21}$ that separates the k bands $p = 1$ and $p = 2$. Such a gap has already been reported in Ref. [16] for the extreme situation of only electric modulation ($m_\mu = 0$). The gap increases with the difference $|m_\varepsilon - m_\mu|$, as has been found in Eq. (25) for weak modulations. We observe that there also exists a very narrow

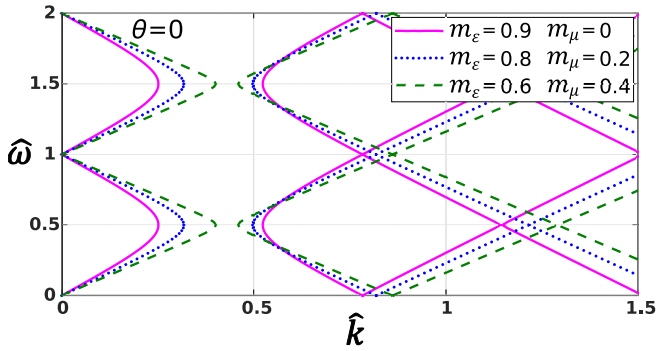

FIG. 1. Photonic band structures for different modulations $m_\varepsilon \neq m_\mu$ with $\varepsilon(t)$ and $\mu(t)$ in phase ($\theta = 0$).

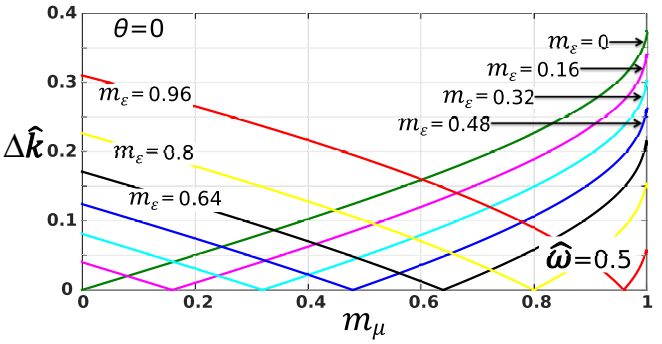

FIG. 3. Variation of first forbidden band gap with m_μ and m_ε assuming the $\varepsilon(t)$ and $\mu(t)$ are in phase ($\theta = 0$).

gap $\Delta\hat{k}_{43}$ between the bands $p = 3$ and $p = 4$; however, it is not perceptible on the scale of the figure. Also note that the modulations m_ε and m_μ are interchangeable, as we have seen from Eq. (19).

Surprisingly, there is a qualitative change in the behavior for equal modulations, $m_\varepsilon = m_\mu \equiv m$, even for very strong modulations, $m \lesssim 1$. The band structure is now constituted by a series of almost straight lines, as seen in Fig. 2. The slopes of these lines rapidly increase with m and the group velocity becomes infinite in the limit $m \to 1$. On the other hand, in the limit $m \to 0$ the dispersion reduces to the empty *temporal* lattice model discussed at the beginning of Sec. III. There are no k gaps for equal modulations.

Figure 3 compactly summarizes the dependencies of the size of the gap $\Delta\hat{k}_{21}$ on the modulations m_ε and m_μ for $\theta = 0$. As $|m_\varepsilon - m_\mu|$ increases, the increase in $\Delta\hat{k}_{21}$ becomes stronger than linear.

The vanishing of the band gap for $m_\varepsilon = m_\mu$ no longer holds true if $\theta \neq 0$, as is manifest in Fig. 4 for three values of the phase difference. The dependence of the normalized gap $\Delta\hat{k}$ on θ is shown in Fig. 5 for a series of values of the modulation. It is interesting to make comparisons with the weak modulation approximation, Eq. (24), which, for equal modulations, reduces to $\Delta k/\bar{k} \simeq m \sin(\frac{1}{2}\theta)$. Clearly, this sinusoidal behavior is confirmed even for $m \simeq 1$.

How good in practice is the approximation presented in Sec. III for weak modulations ($m_{\varepsilon,\mu} \ll 1$)? This question is answered in Tables I–III, where we compare the approximate results for the band gap and the midgap point with accurate numerical solutions of Eq. (28). A close examination of these Tables reveals that Eqs. (23)–(27) give reasonable results even for substantial values of m_ε and m_μ.

B. Lossy medium

Now we allow for losses in our dynamic medium, assuming that the permittivity and permeability have the (constant) imaginary parts ε'' and μ''. The real parts are still modeled according to Eqs. (16) and (17); thus

$$\varepsilon_r(t) = \bar{\varepsilon}_r[1 + m_\varepsilon \sin(\Omega t)] + i\varepsilon_r'', \tag{32}$$

$$\mu_r(t) = \bar{\mu}_r[1 + m_\mu \sin(\Omega t + \theta)] + i\mu_r''. \tag{33}$$

The frequency $\hat{\omega}$ being real, the solutions of Eq. (28) for the wave vector $\hat{k}$ now become complex. In Figs. 6(a) and 6(b) we present, respectively, $\mathrm{Re}\hat{k}(\hat{\omega})$ and $\mathrm{Im}\hat{k}(\hat{\omega})$ for electric modulation ($m_\mu = 0$). We see that $\mathrm{Re}\hat{k}$ increases with $\varepsilon_r''/\varepsilon_r'$ and μ_r''/μ_r', but more so for the first ($p = 1$) band than the second ($p = 2$) band; as a result, the gap $\Delta\hat{k}_{21}$ decreases. We also note that the dispersions for both $\mathrm{Re}\hat{k}$ and $\mathrm{Im}\hat{k}$ remain unaltered if m_ε and m_μ are interchanged, as we saw for real ε and μ. On the other hand, the values of $\varepsilon_r''/\varepsilon_r'$ and μ_r''/μ_r' are not interchangeable. As for $\mathrm{Im}\hat{k}$, it is interesting that it can be greater for the first band than for the second band, giving rise to the loops seen in Fig. 6(b).

For equal modulations, $m_\varepsilon = m_\mu$, there is a remarkable change in comparison to Fig. 2. Namely, the degeneracy at the first point of mode intersections is lifted and a gap is

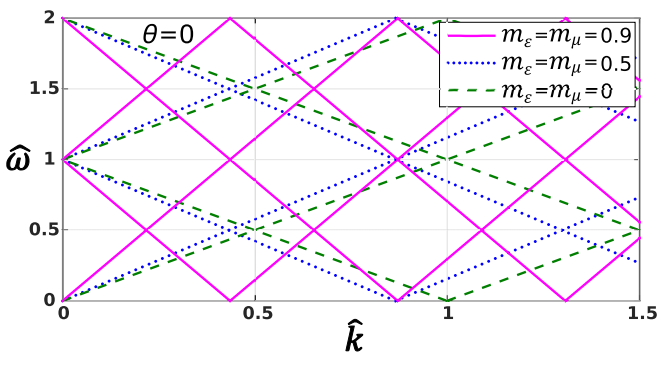

FIG. 2. Same as Fig. 1 for equal modulations, $m_\varepsilon = m_\mu$.

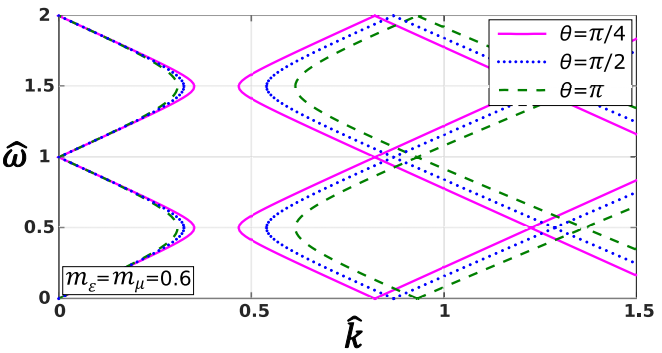

FIG. 4. Photonic band structures for equal modulations, $m_\varepsilon = m_\mu$, and three values of the phase difference θ between $\mu(t)$ and $\varepsilon(t)$.

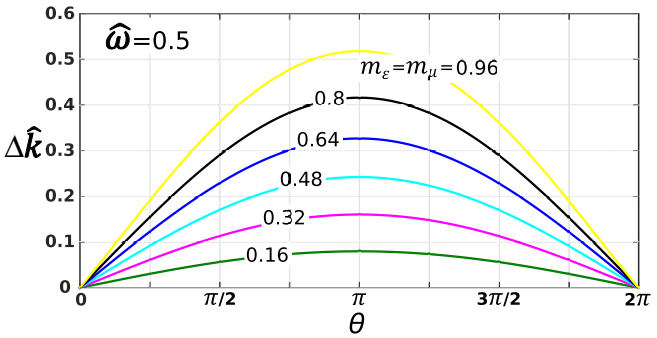

FIG. 5. Variation of first forbidden band gap with θ for $m_\mu = m_\varepsilon$.

created between the bands $p = 1$ and $p = 2$ [see Fig. 7(a)]. Moreover, this gap increases with $\varepsilon_r''/\varepsilon_r'$ and μ_r''/μ_r', contrary to the behavior that we have seen in Fig. 6(a). Another difference is that here $\varepsilon_r''/\varepsilon_r'$ and μ_r''/μ_r' are interchangeable.

V. TRANSMISSION OF LIGHT THROUGH A PLATE WITH MODULATED PERMITTIVITY AND PERMEABILITY

Here, we study the optical response of a slab whose permittivity and permeability are periodically modulated in time. As in the former sections, the mechanism of modulation is not considered explicitly. The relative permittivity and permeability are expanded in a Fourier series, Eqs. (4) and (5); their values on the left (right) sides of the plate are ϵ_1 and μ_1 (ϵ_2 and μ_2). We wish to calculate the reflection and transmission coefficients for normal incidence at a plate of thickness D occupying the region $0 \leqslant x \leqslant D$.

The electric and magnetic fields of the incident plane harmonic wave are

$$E_{\rm inc} = E_0 e^{i[k_0(\omega)x-\omega t]}, \tag{34}$$

$$H_{\rm inc} = H_0 e^{i[k_0(\omega)x-\omega t]}, \tag{35}$$

where $k_0 = (\epsilon_1\mu_1)^{1/2}\omega/c$. The fields in the slab are superpositions of plane waves propagating in the positive and negative directions of the x axis with wave vectors $\pm k_p(\omega)$ ($p = 1,2,3,\ldots$). The dispersion relation $k_p(\omega)$ is still determined from the solution of the eigenvalue equation, Eq. (28). The temporal dependence of these fields obeys the Bloch-Floquet theorem, as in Eq. (6):

$$E_{\rm sl}(x,t) = \sum_{n=-\infty}^{\infty}\sum_{p=1}^{\infty}\left(A_p e^{ik_p(\omega)x} + B_p e^{-ik_p(\omega)x}\right) \times e_{pn}(\omega)e^{-i(\omega-n\Omega)t}, \tag{36}$$

$$H_{\rm sl}(x,t) = \sum_{n=-\infty}^{\infty}\sum_{p=1}^{\infty}\left(C_{pn} e^{ik_p(\omega)x} + D_{pn} e^{-ik_p(\omega)x}\right) \times e_{pn}(\omega)e^{-i(\omega-n\Omega)t}. \tag{37}$$

Here, the eigenfunctions $e_{pn}(\omega)$ also must be found from the solution of the eigenvalue problem. The coefficients A_p, B_p, C_{pn}, and D_{pn} are determined with the help of Faraday's law and the boundary conditions.

The reflected and transmitted waves contain all the harmonics $(\omega - n\Omega)$ $(n = 0, \pm 1, \ldots)$. The reflected fields are

$$E_r = \sum_n E_n^r e^{-i[k_n^r(\omega)x+(\omega-n\Omega)t]}, \tag{38}$$

$$H_r = -\sum_n H_n^r e^{-i[k_n^r(\omega)x+(\omega-n\Omega)t]}, \tag{39}$$

while the transmitted fields are

$$E_t = \sum_n E_n^t e^{i[k_n^t(\omega)(x-D)(\omega-n\Omega)t]}, \tag{40}$$

$$H_t = \sum_n H_n^t e^{i[k_n^t(\omega)(x-D)+(\omega-n\Omega)t]}. \tag{41}$$

Here,

$$k_n^{r,t}(\omega) = (\epsilon_{1,2}\mu_{1,2})^{1/2}(\omega - n\Omega)/c$$

are the wave vectors of the nth harmonic of the reflected and transmitted plane waves. Further, the amplitudes of the electric and magnetic fields in Eqs. (34)–(41) are related by Faraday's law as follows:

$$E_0 = \sqrt{\frac{\mu_0\mu_1}{\varepsilon_0\epsilon_1}}H_0, \quad E_n^{r,t} = \sqrt{\frac{\mu_0\mu_{1,2}}{\varepsilon_0\epsilon_{1,2}}}H_n^{r,t},$$

$$\begin{bmatrix} A_p \\ B_p \end{bmatrix} e_{pn}(\omega) = \sum_m \frac{\mu_0\mu_{n-m}(\omega-n\Omega)e_{pm}(\omega)}{k_p(\omega)}\begin{bmatrix} C_{pm} \\ -D_{pm} \end{bmatrix}. \tag{42}$$

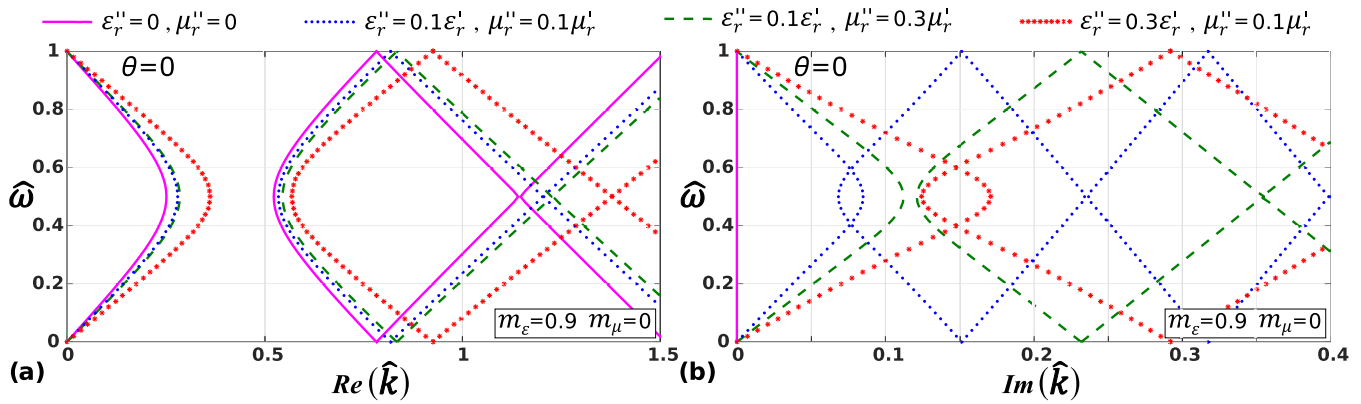

FIG. 6. Real and imaginary parts of the normalized wave vector $\hat{k}$, with $m_\varepsilon = 0.9$, $m_\mu = 0$, and $\theta = 0$ allowing for absorption.

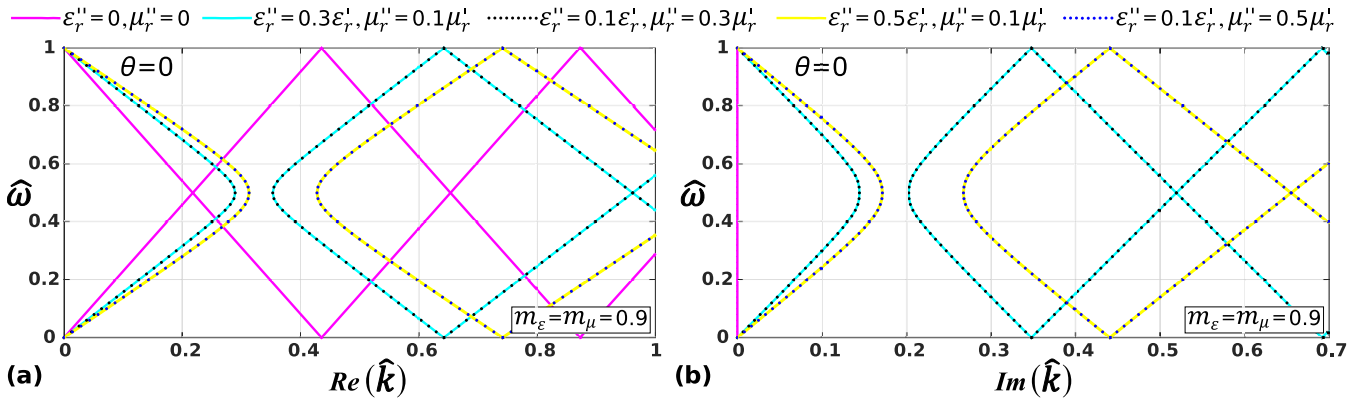

FIG. 7. Same as in Fig. 6 but for equal modulation strengths $m_\varepsilon = m_\mu$.

The boundary conditions imply that the electric and magnetic fields are continuous at the interfaces $x = 0$ and $x = D$ at every instant of time t. With the help of Eqs. (42), we get the following four equations:

$$H_0\delta_{n0} + H_n^r = \sum_{p=1}^{\infty}\sum_m \frac{\mu_0\mu_{n-m}(\omega - n\Omega)}{k_p(\omega)} \times \sqrt{\frac{\varepsilon_0\epsilon_1}{\mu_0\mu_1}}[C_{pm} - D_{pm}]e_{pm}(\omega), \quad (43)$$

$$H_0\delta_{n0} - H_n^r = \sum_{p=1}^{\infty}[C_{pn} + D_{pn}]e_{pn}(\omega), \quad (44)$$

$$H_n^t = \sum_{p=1}^{\infty}\sum_m \frac{\mu_0\mu_{n-m}(\omega - n\Omega)}{k_p(\omega)}\sqrt{\frac{\varepsilon_0\epsilon_2}{\mu_0\mu_2}} \times \left[C_{pm}e^{ik_p(\omega)D} - D_{pm}e^{-ik_p(\omega)D}\right]e_{pm}(\omega), \quad (45)$$

$$H_n^t = \sum_{p=1}^{\infty}\left[C_{pn}e^{ik_p(\omega)D} + D_{pn}e^{-ik_p(\omega)D}\right]e_{pm}(\omega). \quad (46)$$

Now summing Eqs. (43) and (44) and subtracting Eq. (46) from Eq. (45) we obtain

$$\sum_{p=1}^{\infty}\left\{\sum_m \frac{\mu_0\mu_{n-m}(\omega - n\Omega)}{k_p(\omega)}\sqrt{\frac{\varepsilon_0\epsilon_1}{\mu_0\mu_1}}[C_{pm} - D_{pm}]e_{pm}(\omega) + [C_{pn} + D_{pn}]e_{pn}(\omega)\right\} = 2H_0\delta_{n0}, \quad (47)$$

$$\sum_{p=1}^{\infty}\left\{\sum_m \frac{\mu_0\mu_{n-m}(\omega - n\Omega)}{k_p(\omega)}\sqrt{\frac{\varepsilon_0\epsilon_2}{\mu_0\mu_2}} \times \left[C_{pm}e^{ik_p(\omega)D} - D_{pm}e^{-ik_p(\omega)D}\right]e_{pm}(\omega) - \left[C_{pn}e^{ik_p(\omega)D} + D_{pn}e^{-ik_p(\omega)D}\right]e_{pn}(\omega)\right\} = 0. \quad (48)$$

This is an infinite system of inhomogeneous linear equations that can be solved for the unknowns C_{pm}/H_0 and D_{pm}/H_0. The reflection and transmission coefficients for the harmonic $(\omega - n\Omega)$ are then obtained directly from Eqs. (43) and (45):

$$\mathcal{R}_n = \frac{H_n^r}{H_0} = \left(\frac{\varepsilon_0\epsilon_1}{\mu_0\mu_1}\right)^{1/2}\sum_{p=1}^{\infty}\sum_m \frac{\mu_0\mu_{n-m}(\omega - n\Omega)}{k_p(\omega)} \times \left[\frac{C_{pm}}{H_0} - \frac{D_{pm}}{H_0}\right]e_{pm}(\omega) - \delta_{n0}, \quad (49)$$

$$\mathcal{T}_n = \frac{H_n^t}{H_0} = \left(\frac{\varepsilon_0\epsilon_2}{\mu_0\mu_2}\right)^{1/2}\sum_{p=1}^{\infty}\sum_m \frac{\mu_0\mu_{n-m}(\omega - n\Omega)}{k_p(\omega)} \times \left[\frac{C_{pm}}{H_0}e^{ik_p(\omega)D} - \frac{D_{pm}}{H_0}e^{-ik_p(\omega)D}\right]e_{pm}(\omega). \quad (50)$$

Our numerical procedure involved the solution of 105 equations, taking an appropriate number of combinations for the indeces p and m. It also required the solution of the bulk eigenvalue problem, Eq. (28), for both the eigenvalues $\hat{\omega}(k_p)$ and the eigenvectors $e_{pn}(\hat{\omega})$. This resulted in excellent convergence for the transmission coefficients $\mathcal{T}_n(\omega)$. In Figs. 8–11 we present transmission spectra for a dynamic-periodic slab characterized by the normalized thickness:

$$\nu = D\Omega(\bar{\varepsilon}_r\bar{\mu}_r)^{1/2}/c = 2\bar{k}D, \quad (51)$$

where D is the actual thickness and $\bar{k}$ is the midgap wave vector in the limit of vanishing modulation, as defined in Eq. (23). The case of purely electric modulation ($m_\varepsilon \neq 0, m_\mu = 0$) was already explored in Ref. [16]. As pointed out there, for weak modulation ($m_\varepsilon \ll 1$) these spectra can be interpreted as modified Fabry-Perot resonances, with the fundamental ($n = 0$) reflection coefficients vanishing and $\mathcal{T}_0 = 1$ whenever an integer number of half-wavelengths fits in the width of the slab. In the figures that follow we consider combinations of electric and magnetic modulations ($m_\varepsilon \lesssim 1, m_\mu \lesssim 1$) so strong that the Fabry-Perot resonances become unrecognizable.

In Figs. 8 and 9 the electric and magnetic modulations are in phase ($\theta = 0$); they differ in that in Fig. 8 $m_\varepsilon \neq m_\mu$, while in Fig. 9 $m_\varepsilon = m_\mu$. Two normalized thicknesses ($\nu = 1$ *and* $\nu = 4$) are considered. The transmission spectra are shown for the fundamental ($n = 0$) and three harmonics ($n = 0, \pm 1, 2$). These correspond to light transmitted at the frequencies ω, $|\omega \mp \Omega|$, and $|\omega - 2\Omega|$. For $\nu = 1$ there is a qualitative difference between the Figs. 8 and 9; namely, the $\mathcal{T}_n$ vanish at certain frequencies for equal modulations, while

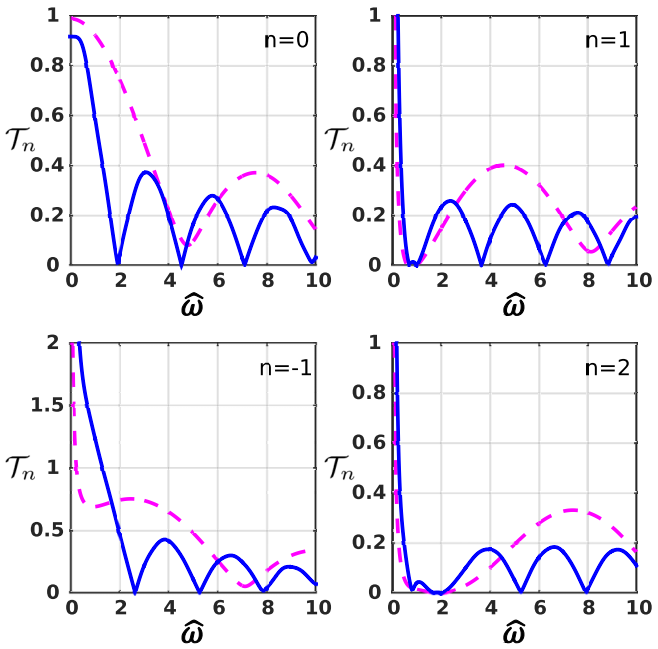

FIG. 8. Transmission spectra $\mathcal{T}_n(\hat{\omega})$ for the fundamental $n = 0$ and the harmonics $n = \pm 1,2$ for two values of the normalized slab thickness: $\nu = 1$ (magenta dash) and $\nu = 4$ (blue solid). The electric and magnetic modulations are assumed to be in phase ($\theta = 0$) and their strengths are $m_\varepsilon = 0.8$ and $m_\mu = 0.2$.

they only exhibit minima if the modulations are different. Also, the number of oscillations is greater for $\nu = 4$ than for $\nu = 1$ because the average number of wavelengths decreases in comparison to the thickness D. Finally $\mathcal{T}_{-1}$, $\mathcal{T}_1$, and $\mathcal{T}_2$ are of the same order as $\mathcal{T}_0$ due to the very strong modulations assumed.

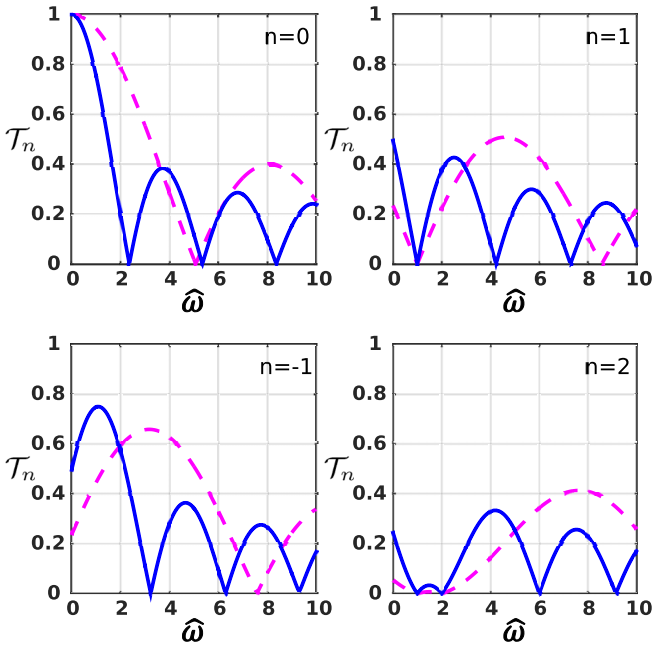

FIG. 9. Same as in Fig. 8 but for equal modulations, $m_\varepsilon = m_\mu = 0.5$.

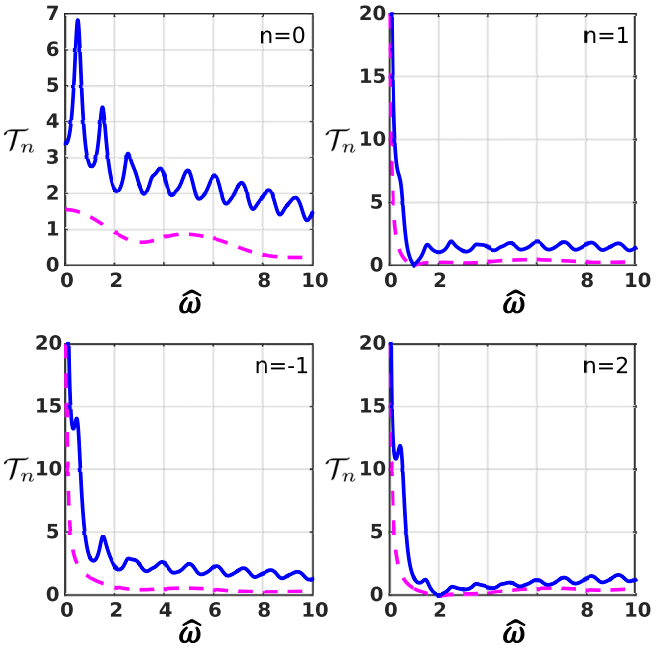

FIG. 10. Same as in Fig. 8 but for equal modulations, $m_\varepsilon = m_\mu = 0.9$, that are out of phase ($\theta = \pi$).

As has been already commented in Ref. [16], ours is an open system that can receive energy from the source of modulation. Hence, the reflection and transmission coefficients can be greater than 1. In the presence of simultaneous electric and magnetic modulations, this effect can be very strong for equal modulations ($m_\varepsilon = m_\mu$) that are out of phase ($\theta = \pi$), as seen in Fig. 10. Curiously, the transmitted harmonics ($\mathcal{T}_{\pm 1}$ and $\mathcal{T}_2$) can be even greater than the transmitted fundamental ($\mathcal{T}_0$). The strong energy gain occurs for the normalized thickness $\nu = 4$, not, however, for $\nu = 1$. Note that the pronounced oscillations peak at, roughly, $\hat{\omega} = 1/2,3/2,5/2,\ldots$, thus suggesting parametric resonances. These have been explored in Ref. [18] for $m_\mu = 0$. The present situation is quite different and merits deeper study, to be undertaken in the future. It seems that Fig. 10 corresponds to a transition from Fabry-Perot resonances to parametric resonances. Figure 11 demonstrates a case of $\mathcal{T}_0(\omega)$ being greatest for $\theta = \pi$ and smallest for $\theta = 0$, with intermediate values for $\theta = \pi/2$.

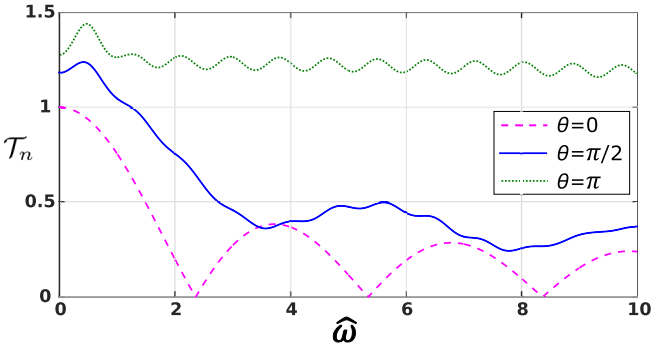

FIG. 11. The fundamental transmission coefficient $\mathcal{T}_{n=0}$ for a normalized thickness $\nu = 4$, equal modulations $m_\varepsilon = m_\mu = 0.5$, and three values of the phase difference: $\theta = 0$, $\pi/2$, and π.

VI. CONCLUSION

The subject of this paper is a generalized *temporal* photonic crystal, assuming periodic modulations in the time of both the permittivity and permeability. For greater versatility, the electric and magnetic modulations can have an arbitrary phase difference. Thus, the photonic band structure $k(\omega)$, obtained from the solution of a complicated eigenvalue problem, depends crucially on whether the two modulations are in phase or out of phase and also on whether the strengths of these modulations are different or equal. It is these differences that lead to the existence or absence of band gaps between the k bands. In addition to the dispersion $k(\omega)$ of the waves we also studied their damping and transmission through a dynamic slab. A particular case of transmission spectra suggests the onset of parametric resonances, meriting further investigation. The fact that k gaps were recently measured and reported [20] in a transmission line with periodically modulated capacitors implies that, by modulating the inductors as well, the behavior and effects predicted here can be reproduced at radio, microwave, and even THz frequencies. We also anticipate analogous effects in periodically modulated elastic ("phononic"), plasmonic, and other systems.

[1] M. Uhlmann, G. Plunien, R. Schützhold, and G. Soff, Phys. Rev. Lett. **93**, 193601 (2004).

[2] M. F. Yanik and S. Fan, Phys. Rev. Lett. **92**, 083901 (2004); **93**, 173903 (2004); S. Longhi, Phys. Rev. E **75**, 026606 (2007); Y. Sivan and J. B. Pendry, Phys. Rev. Lett. **106**, 193902 (2011); Phys. Rev. A **84**, 033822 (2011).

[3] Z. Yu and S. Fan, Nat. Photonics **3**, 91 (2009); N. H. Lindner, G. Rafael, and V. Galitski, Nat. Phys. **7**, 490 (2011); N. A. Estep, D. L. Sounas, J. Soric, and A. Alù, *ibid.* **10**, 923 (2014).

[4] L. Yuan and S. Fan, Phys. Rev. Lett. **114**, 243901 (2015); Phys. Rev. A **92**, 053822 (2015).

[5] P. Dong, S. F. Preble, J. T. Robinson, S. Manipatruni, and M. Lipson, Phys. Rev. Lett. **100**, 033904 (2008).

[6] K. Fang, Z. Yu, and S. Fan, Phys. Rev. Lett. **108**, 153901 (2012).

[7] W. J. Padilla, A. J. Taylor, C. Highstrete, Mark Lee, and R. D. Averitt, Phys. Rev. Lett. **96**, 107401 (2006); V. J. Logeeswaran, A. N. Stameroff, M. Saif Islam, W. Wu, A. M. Bratkovsky, P. J. Kuekes, S. Y. Wang, and R. S. Williams, Appl. Phys. A **87**, 209 (2007).

[8] A. R. Katko, S. Gu, J. P. Barrett, B.-I. Popa, G. Shvets, and S. A. Cummer, Phys. Rev. Lett. **105**, 123905 (2010).

[9] E. Poutrina, S. Larouche, and D. R. Smith, Opt. Commun. **283**, 1640 (2010).

[10] M. Artamonov and T. Seideman, J. Phys. Chem. Lett. **6**, 320 (2015).

[11] A. D. Boardman, V. V. Grimalsky, Y. S. Kivshar, S. V. Koshevaya, M. Lapine, N. M. Litchinitser, V. N. Malnev, M. Noginov, Y. G. Rapoport, and V. M. Shalaev, Laser Photonics Rev. **5**, 287 (2011); A. Q. Liu, W. M. Zhu, D. P. Tsai, and N. I. Zheludev, J. Opt. **14**, 114009 (2012); M. Rahm, J.-S. Li, and W. J. Padilla, J. Infrared Millimeter Terahertz Waves **34**, 1 (2013); M. Lapine, I. V. Shadrivov, and Y. S. Kivshar, Rev. Mod. Phys. **86**, 1093 (2014).

[12] A. B. Kozyrev, H. Kim, and D. W. van der Weide, Appl. Phys. Lett. **88**, 264101 (2006).

[13] A. B. Kozyrev and D. W. van der Weide, J. Phys. D: Appl. Phys. **41**, 173001 (2008).

[14] L. Q. English, F. Palmero, P. Candiani, J. Cuevas, R. Carretero-Gonzalez, P. G. Kevrekidis, and A. J. Sievers, Phys. Rev. Lett. **108**, 084101 (2012).

[15] M. Gorkunov and M. Lapine, Phys. Rev. B **70**, 235109 (2004).

[16] J. R. Zurita-Sánchez, P. Halevi, and J. C. Cervantes-González, Phys. Rev. A **79**, 053821 (2009).

[17] B. Wang, J. Teng, and X. Yuan, Appl. Phys. Lett. **98**, 263111 (2011); Appl. Phys. A **107**, 43 (2012).

[18] J. R. Zurita-Sánchez and P. Halevi, Phys. Rev. A **81**, 053834 (2010).

[19] J. R. Zurita-Sánchez, J. H. Abundis-Patiño, and P. Halevi, Opt. Express **20**, 5586 (2012).

[20] J. R. Reyes-Ayona and P. Halevi, Appl. Phys. Lett. **107**, 074101 (2015).

[21] J. R. Reyes-Ayona and P. Halevi (unpublished).

[22] C. Kittel, *Introduction to Solid State Physics* (Wiley & Sons, New York, 2005).